Performance of a Forward Swept Wing Fighter Utilizing Thrust Vectoring and Reversing

Eugene H. Miller*
Grumman Aerospace Corporation, Bethpage, New York

Many studies have been performed demonstrating the benefits of two-dimensional nozzles with thrust vectoring. These include STOL characteristics, maneuverability, and reduced drag. Grumman performed a study to determine the adaptability of the General Electric Augmented Deflector Exhaust Nozzle (ADEN) to their forward swept wing (X-29) aircraft and to provide a manned flight demonstrator of two-dimensional nozzle technology. A thrust reverser was also examined, along with other options. The study concluded that incorporations of the ADEN nozzle alone and together with a thrust reverser are feasible in the X-29 aircraft. The main performance advantages resulted in a 48% decrease in takeoff ground roll, a 7% decrease in landing ground roll, and a 4% increase in instantaneous turn rate. Incorporation of a thrust reverser produced a 30% reduction in landing distance in addition to the tactical advantages that can be provided with in-flight deceleration.

Nomenclature

A/B	= afterburner
ADEN	= Augmented Deflector Exhaust Nozzle
A_8	= nozzle throat area
C_{fg}	= nozzle gross thrust coefficient
C_{fgr}	= resultant nozzle gross thrust coefficient
c.g.	= center of gravity
C_T	= net thrust coefficient
DARPA	= Defense Advanced Research Projects Agency
ECU	= electrical control unit
FS	= fuselage station
FSW	= forward swept wing
F_G	= gross thrust
g	= acceleration normalized by acceleration due to gravity
INT	= intermediate power setting
IRP	= intermediate rated power
M	= Mach number
NAPC	= Naval Air Propulsion Center
NPR	= nozzle pressure ratio
PLA	= power lever angle
SERN	= single-expansion ramp nozzle
SL	= sea level
S_{REF}	= wing reference area
TR	= thrust reverser
VEER	= variable external expansion ramp
V_{MNU}	= minimum nosewheel unstick, nosewheel liftoff velocity
W	= aircraft gross weight
α	= angle of attack
δ_c	= canard deflection angle
δ_j	= gross thrust or jet deflection angle, measured from fuselage waterline
θ_v	= VEER deflection angle, measured from fuselage waterline

Presented as Paper 83-2482 at the AIAA Aircraft Design Systems and Operations Meeting, Fort Worth, TX, Oct. 17-19, 1983; received Feb. 10, 1985; revision received Sept. 9, 1985.

*Engineering Specialist.

Introduction

NONAXISYMMETRIC nozzles have been recognized for their superior adaptability in certain types of aircraft installations. The benefits to advanced propulsion systems appear in the general form of improved installed performance, aircraft maneuverability, and STOL characteristics. Several programs sponsored by NASA and other federal agencies have begun to develop the necessary technology base that will allow verification and quantification of analytically indicated benefits. One of the most important of these programs was the V/STOL nozzle program sponsored by the Naval Air Propulsion Center (NAPC). Under this program, a full-scale ADEN was conceived, designed, built, and tested on a YJ-101 engine. The tests were run at sea level, static conditions at the General Electric (GE) test facility in Peebles, Ohio. Following the YJ-101/ADEN test program at Peebles, the same engine and nozzle were tested by the Navy at its Lakehurst test facility to evaluate infrared radiation signature characteristics of the ADEN. The tests were run at dry power settings and sea level, static conditions. These sea level tests were recently followed by an altitude test program[1] at the NASA Lewis Research Center at the request of the Navy. The tests were conducted using the existing ADEN mounted behind an F404 engine. The test conditions included dry and A/B operation at nozzle pressure ratios up to 15.0. Thrust vectoring was demonstrated using the VEER settings up to ± 15 deg for both dry and A/B conditions. These three tests accumulated a total of 151 h of test time with 28 h of A/B operation.

The objective of the study highlighted in this paper[2,3] was to determine installation feasibility for the incorporation of a GE ADEN on the F404-GE-400 powerplant (the engine installed in the Grumman X-29 FSW aircraft) to provide a manned flight demonstrator of two-dimensional nozzle technology. In addition, the study also provided definition of the modifications to the existing ADEN and F404 engine hardware to accommodate a thrust reverser (TR). Key features of the TR include 50% IRP reverse thrust, four ports, ADEN ventral flap blocker, and a unique reverser actuation system.

Configuration Design

The basic X-29 forward swept wing aircraft is shown in Fig. 1 and described in Refs. 4 and 5. The aircraft is a "technology demonstrator" designed to incorporate advanced composites, variable camber, relaxed static stability, close-coupled canard, and a thin supercritical wing. The current study examines the adaptability of this aircraft with an axisymmetric nozzle to a modified two-dimensional, vectoring ADEN nozzle. The region of the X-29 modified to incorporate the ADEN nozzle is depicted by cross hatching in Fig. 1. Although no performance goals or mission requirements were specified for the study, design requirements were established that retain the baseline X-29 capabilities. Additional requirements were:

1) thrust vector range: -15 to $+30$ deg for $M<1.2$ and ± 10 deg for $M>1.2$

2) maximum vectoring range applies for dry and A/B power settings.

Modifications to the existing GE ADEN include removal of the deflector hood and its operating mechanism. A flight hardware VEER will be developed commensurate with airframe geometry and operational requirements (i.e., to match the fuselage air passage and internal nozzle ramp contours, and deflection rates). A dual-tandem actuator is proposed to provide adequate control power for the VEER design rates for full engine thrust throughout the design flight envelope, while also providing flight control system redundancy. The existing rear mount on the F404 engine was moved aft to the nozzle transition section to provide vertical load support. Vectored thrust load reactions are transmitted to the forward main mounts by providing adequate bending stiffness in the engine case; the aft mount takes only vertical loads.

Engine modifications to accommodate the TR primarily involve a new augmentor case design and a new mechanism to operate the throat ramp. Doors to the fuselage and augmentor to duct the reverse flow are interconnected by a hydraulically actuated linkage driven by the engine. The ventral flap is used to block the main exhaust flow, thereby eliminating the need for a separate TR blocker.

No ballast requirements were deemed necessary for the X-29/ADEN configuration. However, 263 lb of ballast was required in the nose for the X-29/ADEN + TR configuration to constrain c.g. travel within acceptable limits.

Mechanization of the flight control system to provide power and control of the VEER includes triple-redundant control electronics to drive a quad-servo actuator. The remotely installed servo actuator drives the VEER dual-tandem power actuator mounted on the engine hood structure. The redundancy provides a fail-operational capability for takeoff and landing safety. VEER control electronics can be accommodated in the existing flight control computers.

Control of the VEER for test purposes is via the existing computer command control panel, which allows selection of preprogrammed software options. A VEER trim switch in the instrument panel provides pilot control of the VEER trim position. A cockpit VEER engage switch completes the VEER control implementation.

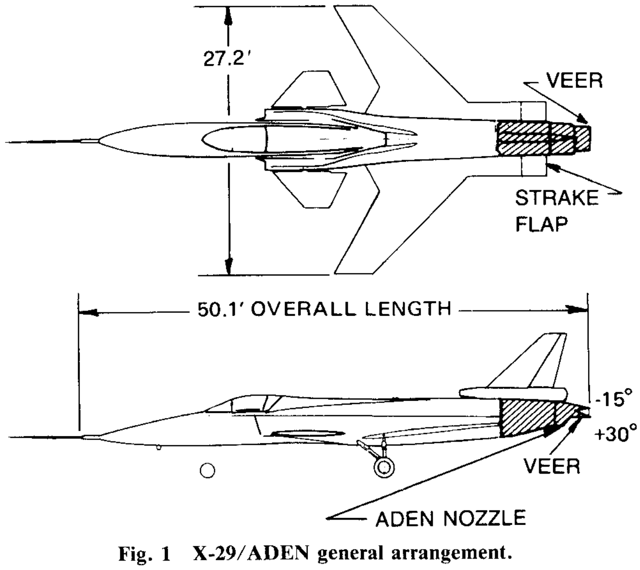

Fig. 1 X-29/ADEN general arrangement.

X-29/ADEN

The baseline F404 engine has an axisymmetric convergent-divergent exhaust nozzle to provide the correct exit area for the engine and to efficiently expand the exhaust gases for maximum thrust. Substitution of a two-dimensional asymmetric ADEN could result in the significant flight operational benefits that can be derived from a thrust vectoring nozzle.

The ADEN exhaust system is a nonaxisymmetric, external expansion-type cruise nozzle with area variation by convergent and divergent variable flaps. A VEER is provided for flight maneuver control and a variable ventral flap, located downstream of the throat, varies the nozzle internal area ratio as required over the range of operating pressure ratios. Nozzle area control in the cruise mode is provided by varying the convergent and divergent flaps that are hinge connected at the throat. The forward end of the convergent flap is attached to a drive shaft positioned by hydraulic actuators and drive cranks attached to each end of the shafts. The ventral flap is operated by the nozzle area control logic by means of a cam and push rod mechanism. Thrust vector angle control in the original ADEN was accomplished by rotating the bonnet-type deflector downward by use of a conventional aircraft hydraulic actuator.

The ADEN was designed as a V/STOL nozzle with a thrust vectoring capability from 0 to over 90 deg down. For V/STOL operation, a rotating bonnet-type deflector was used to deflect the jet downward. Since the X-29/ADEN design requirements are -15 to $+30$ deg of vectoring, the ADEN deflector was removed and thrust vectoring accomplished by a modulated VEER. This resulted in reduced weight because the deflector, cooling tubes, actuators, and associated linkages were removed. Design of the VEER cooling system ducts is also simplified by removing the deflector. With removal of the deflector, a redesigned VEER is mounted to the ADEN. The vectored position of the VEER will have no significant effect

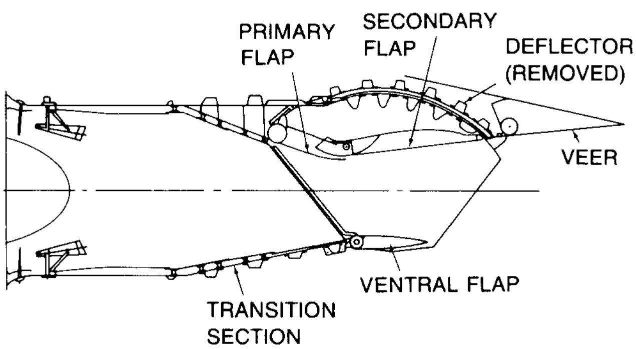

Fig. 2 ADEN flowpath and basic design.

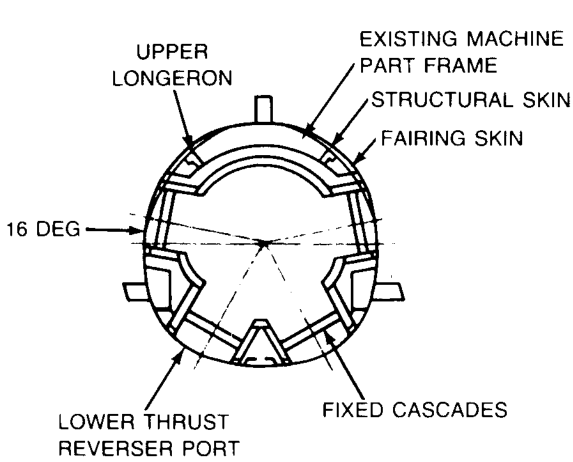

Fig. 3 X-29/ADEN thrust reverser installation.

on the operating characteristics of the engine because the VEER is downstream of the nozzle throat.

A cross section of the nozzle, shown in Fig. 2, depicts the exhaust duct transition from round to rectangular and the rectangular flowpath cross section in the A/B mode. The existing ADEN was designed for use with the YJ-101 engine from which the F404 was derived and, with some minor exceptions, is therefore generally compatible with the F404. Relocation of the rear mount will reduce the bending moments induced into the engine casings under flight and maneuver loads.

Thrust Reverser

A design study was conducted to provide conceptual definition of a thrust reverser. This study considered location and design of the reverse flow exhaust ports, primary exhaust flow blocker, actuation system, as well as installation procedures. A key objective was integration of the reverser within the airframe, with minimum change to the existing structure. The results of this study included: 1) concept capable of 50% IRP reverse thrust; 2) four-port design; 3) added actuation system for the ventral flap, allowing it to provide a blocker function; 4) thrust reverser actuation system to coordinate all four ports; and 5) unchanged F404/ADEN mount arrangement.

The choice of location and placement of ports is limited by existing aircraft structure. This results in the reverser operating close to the A/B flameholders, with accompanying wake effects. Aircraft structure limits the shape and size of port entry and exit.

The developed TR concept satisfies the above requirements. The installation drawing in Fig. 3 illustrates the concept definition. The port size shown reflects the effects of port shape, blocker location, wakes, flow blockage, and angularity effects on flow coefficient. The mechanical design and actuation system reflects the requirements for practical installation and removal of the propulsion system, as well as providing access for maintenance while minimizing weight and complexity.

The four-port concept is designed for dry power operation. Exterior doors provide a smooth aerodynamic contour when closed; an inner slide valve and door provide a smooth internal exhaust contour when closed and allow the air to flow through the ports when open. The ADEN ventral flap also serves as a blocker door and is coordinated with the TR and primary flap to maintain a constant effective exhaust area during TR deployment. Each port has a fixed turning cascade and two outer doors that match aircraft contours and are actuated by a common actuation ring. To minimize costs, the cascade assembly is common to all four ports. Each door has a different contour corresponding to the X-29's external contours and requiring a unique design.

Addition of a TR to the F404/ADEN adds significantly to the controls and actuation systems. First, because of its new blocker function, the ADEN ventral flap is no longer linked to the primary flap and will require a separate pair of actuators. Second, the reverser will require its own set of actuators. Third, the control system will need the added capacity to control and coordinate these actuators with each other and with the A_8 actuators.

Changes to accommodate these additions in the F404 nozzle control system impact the hydraulic pump and the ECU. The nozzle hydraulic pump, which is currently a servo pump dedicated to the A_8 actuation system, will be replaced by a variable-displacement, constant-pressure pump capable of supplying the three separate actuation systems. Additions are also necessary in the ECU to schedule and coordinate the primary flap and ventral flap.

The avoid nose pitch-down moments with accompanying large impact forces on the nose gear, the TR will be interlocked to prevent activation until nosewheel touchdown. At this time, the reverser ports will be opened and the engine will be spooled-up to full intermediate power where it remains until a cutoff speed of 40 knots.

In the thrust reversing mode, estimated performance is 50% of intermediate rated power. This accounts for leakage past the nozzle seals, as well as past the tip of the ventral flap/blocker.

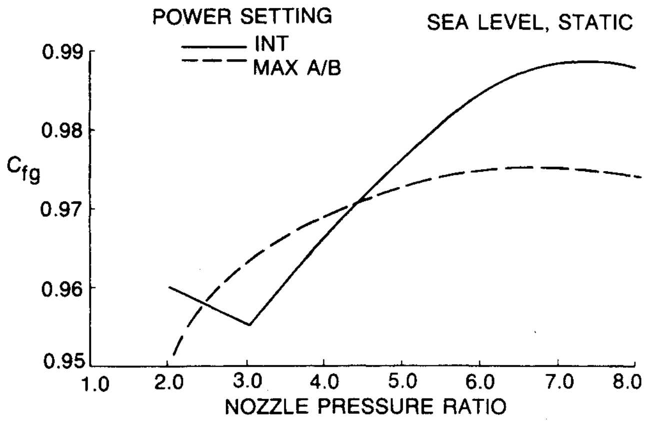

Fig. 4 ADEN thrust coefficients vs nozzle pressure ratio.

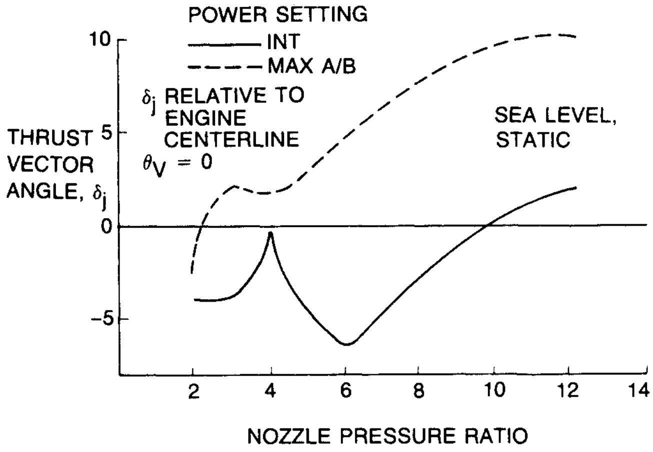

Fig. 5 ADEN thrust vector angle vs nozzle pressure ratio.

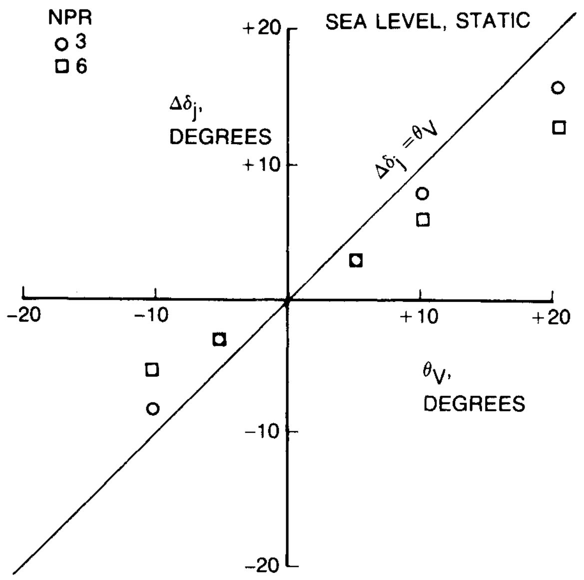

Fig. 6 Change of ADEN thrust angle vs VEER deflection angle.

Propulsion Methodology

The starting point of the propulsion methodology is the output from the GE engine customer deck for the F404-GE-400. First, the axisymmetric nozzle performance incorporated in the deck is replaced by ADEN thrust coefficients. These coefficients are functions of NPR and A_8. Second, the thrust angle δ_j is determined. Because the ADEN is a single-expansion ramp nozzle (SERN), asymmetric forces exist on the upper ramp. The thrust vector angle is a function of NPR and A_8. Third, the thrust magnitude and angle corrections due to vectoring the VEER are determined. The thrust magnitude corrections (ΔC_{fg_r}) are a function of the VEER angle (θ_v) and power setting (NPR). The thrust deflection angle corrections ($\Delta\delta_j$) are also a function of the VEER angle and power setting.

The thrust coefficients utilized in the X-29/ADEN analysis are presented in Fig. 4. Performance data for the intermediate and maximum A/B power settings are shown in the figure.

Thrust vector angle δ_j vs nozzle pressure ratio is shown in Fig. 5 for intermediate and maximum A/B power settings. Note that the intermediate power setting data presents a sharp spike at an NPR of approximately 4.0 and that all values of the thrust vector angle are negative below an NPR of 10.0. The maximum A/B data present a much smoother initial peak; at maximum A/B, the thrust vector angles are positive above NPR = 2.2. Above NPR values of 6.0, both power settings present a generally increased thrust vector angle with NPR.

The changes in thrust vector angle $\Delta\delta_j$ with VEER angle θ_v are shown in Fig. 6. It is seen that when the VEER vectors +20 deg, at an NPR of 3, the jet vectors approximately 70% of this value. The exact value of $\Delta\delta_j$ is highly dependent on nozzle pressure ratio and can even provide values of $\Delta\delta_j$ equal to (or slightly greater than) θ_v at some points (NPR $\approx$ 4.0).

The change in thrust ΔC_{fg_r} with VEER angle θ_v is shown in Fig. 7. Note that as the VEER angle increases, thrust changes result due to turning losses in the main flow. These changes are losses which are the result of shocks in the supersonic exhaust flow as the VEER vectors down through positive angles. These losses are also a function of NPR. As the VEER vectors up through negative angles, there can be an improvement in thrust performance over the baseline as the nozzle geometry (i.e., ramp geometry) changes.

The optimization of axial thrust is shown in Fig. 8 for Mach 0.2, sea level, and various power settings (PLA). The cosine of the jet angle multiplied by the gross thrust provided the axial thrust component. It is seen that the axial thrust component maximizes at −2.5 deg VEER angle for intermediate power (PLA = 90). For maximum A/B (PLA = 130), the axial thrust optimizes at a VEER angle of −5 deg.

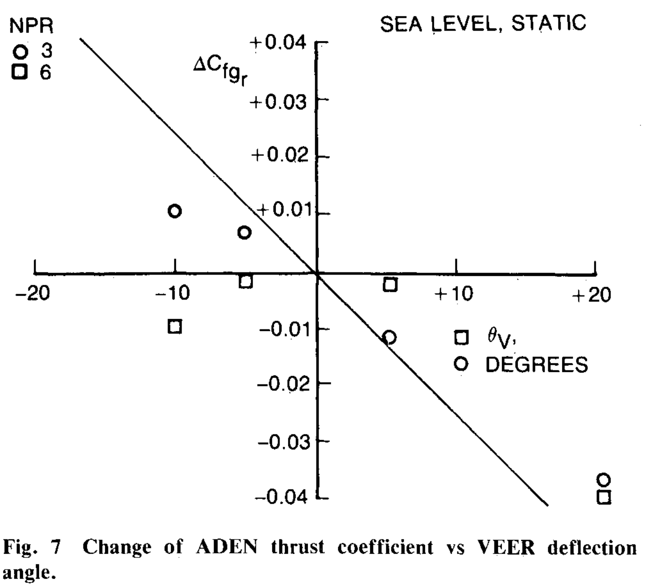

Fig. 7 Change of ADEN thrust coefficient vs VEER deflection angle.

Nozzle/Afterbody Integration

The ADEN nozzle installation in the X-29 is illustrated in Fig. 9. Determination of the contours and estimation of the aft-end drag for the X-29/ADEN aft-end were examined analytically using Grumman's transonic/supersonic boattail code (GAC-BOAT).[6-8] In this code, the freestream flowfield is determined by a "patchwork" approach. Each patched region is iteratively solved with all its neighboring regions until the convergence limits are satisfied. The code also patches a boundary layer, includes a supersonic exhaust plume, incorporates a separation analysis, and takes into account mass entrainment due to the plume mixing region.

Results of the analysis for the axisymmetric and ADEN nozzles are seen in Fig. 10. Nozzle/afterbody drag is shown in the figure as a function of Mach number. Both intermediate and maximum A/B power settings are given for the axisymmetric and ADEN nozzles. Typical drag curves are displayed for both nozzles (i.e., a slight decrease in drag subsonically followed by a drag rise peaking at Mach 1.2 and then a decrease in drag). For the axisymmetric nozzle, the back-end

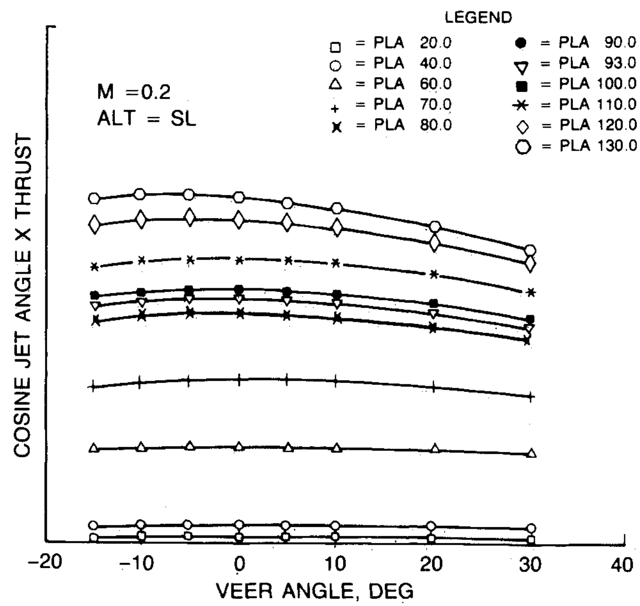

Fig. 8 Thrust optimization.

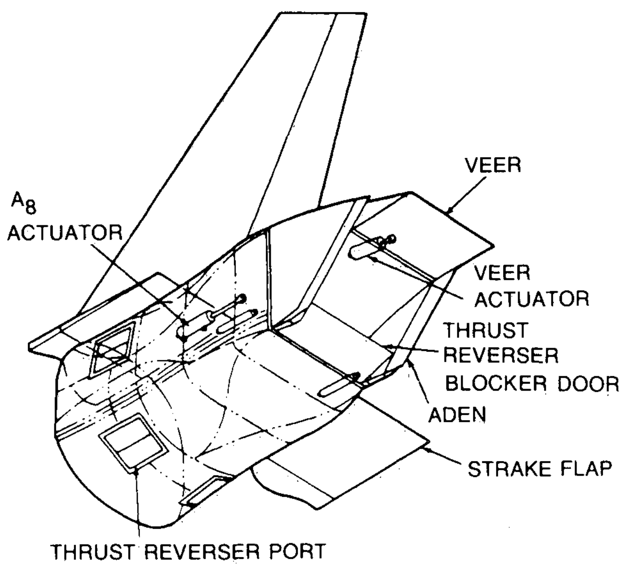

Fig. 9 X-29/ADEN installation.

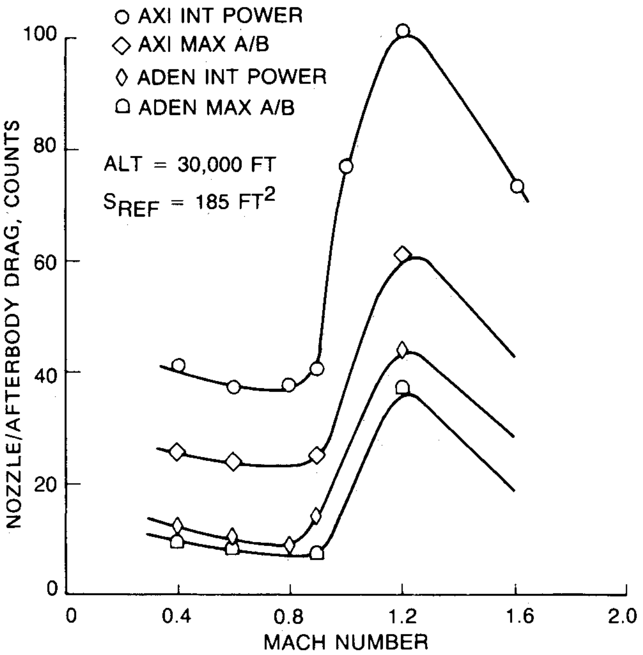

Fig. 10 Nozzle/afterbody drag comparison.

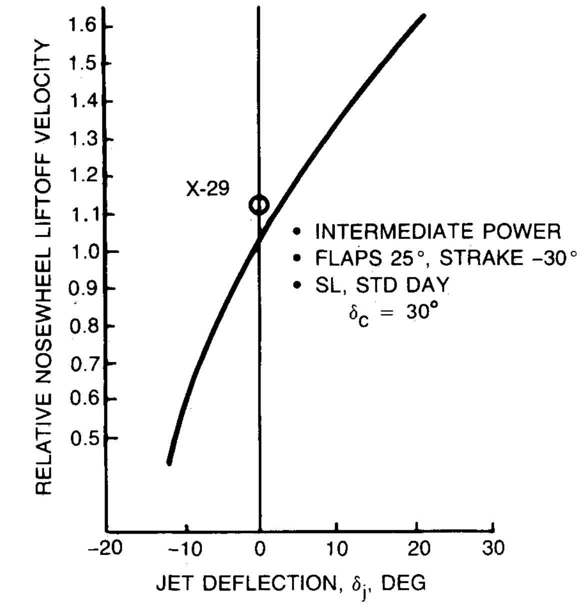

Fig. 11 Effect of thrust vectoring on nosewheel liftoff speed.

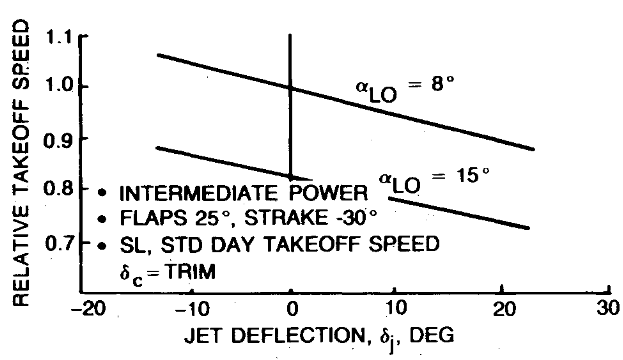

Fig. 12 Effect of thrust vectoring on takeoff speed.

drag is 15.5 counts greater for the intermediate power configuration than the afterburning at Mach 0.9, 30,000 ft. There is also a decrease in aft-end drag with the ADEN nozzle when going from intermediate power to maximum A/B. At Mach 0.9, 30,000 ft, this decrease is 7 counts. The aft-end drag for the ADEN is lower than that for the axisymmetric nozzle: 26 counts at intermediate power Mach 0.9, and 18 counts at maximum A/B Mach 0.9.

Similar trends were calculated by utilizing a wave drag computer code. The calculations were performed by examining the aircraft aft-end up to the aircraft customer connect station. The decrease in supersonic drag is due to reduced afterbody closure, resulting from refairing the fuselage to a rectangular cross section of somewhat increased area.

The analytic results are somewhat similar to the wind tunnel trends in Refs. 9 and 10, which tested two-dimensional nozzles including the ADEN together with a baseline axisymmetric nozzle on a powered scale model of the F-18 aircraft. Results of the wind tunnel program resulted in reductions of afterbody drag, by incorporation of the ADEN nozzle in place of the axisymmetric nozzle, as large as 58 counts at Mach 0.60, and 12 counts at Mach 1.20 for the dry power configuration.

Performance

ADEN installation and integration in the X-29 offer attractive performance advantages. These advantages occur primarily in flight regimes characterized by low dynamic pressure (i.e., low airspeed), such as takeoff, approach/landing, and high angle-of-attack maneuvering. Improvements in performance are attributable to the benefits of direct propulsive lift and enhanced pitch authority from thrust vectoring. The most appreciable gain is a substantial improvement in takeoff performance resulting from the use of thrust vectoring to initiate rotation of the X-29/ADEN with upward VEER deflection, followed by downward VEER deflection until the aircraft lifts off.

Thrust vectoring also leads to a reduction in approach speed and corresponding landing ground roll, slightly improved instantaneous turning performance, and increased pitch control power: particularly at low-q, high-α conditions. No benefits, however, are noted in sustained maneuver performance from thrust vectoring. Reductions in cruise trim drag, both subsonic and supersonic, are achievable with vectored thrust.

The addition of thrust reversing on the X-29 leads to significantly reduced landing distances, tactical advantages through improved deceleration capability in level flight, and increased constant speed dive angle.

Takeoff

The most appreciable gain from the use of thrust vectoring on the X-29 is improved takeoff performance. Comparison of maximum power takeoff characteristics at full-fuel gross weights shows that the X-29/ADEN has a potential field length representing moderate STOL levels. The X-29 without thrust vectoring capability uses almost twice the runway length before liftoff. The reason for this apparent "quantum leap" in takeoff performance is that the basic X-29 has a high minimum nosewheel liftoff speed, primarily due to the forward location of the c.g. when fully fueled.

The high velocity necessary to initiate X-29 rotation is also caused by a large nose-down moment due to thrust and, to a lesser extent, by the negative pitching moment shift due to the 25 deg wing flap deflection. On the other hand, the X-29/ADEN has the ability to initiate rotation during the takeoff ground run at very low airspeeds. Upward jet deflection of 10 deg reduces minimum rotation speed by 46% at intermediate thrust, while downward jet deflection increases V_{MNU} (see Fig. 11). Note in Fig. 11 that the X-29 has a V_{MNU} 8.7% greater than the unvectored X-29/ADEN. This is due to the differences in c.g. location when fully fueled, with the X-29/ADEN c.g. 5 in. further aft.

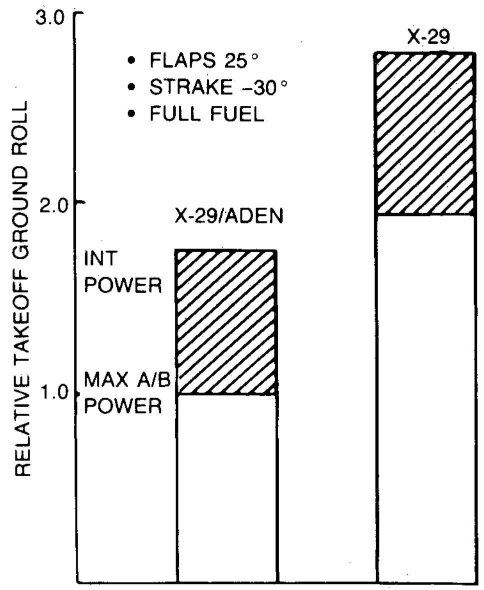

Fig. 13 Comparison of takeoff distance.

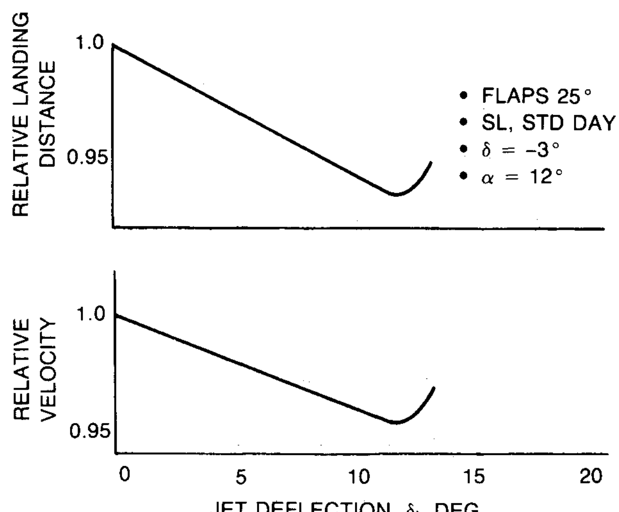

Fig. 14 Effect of thrust vectoring on approach speed and landing distance.

The forward swept wing of the X-29 provides sufficient high lift to enable flight at relatively low airspeeds. Due to the requisite high velocity for nosewheel unstick, however, the X-29 lifts off shortly after the nosewheel leaves the ground at about 8 deg angle of attack. Thrust vectoring to initiate rotation allows the X-29/ADEN to exploit the high-lift characteristics of the FSW. Takeoff becomes possible near the tail-scrape limit of 15 deg pitch attitude, which results in liftoff speeds approximately 18% less than at 8 deg (see Fig. 12). As the graph indicates, takeoff speed can be further reduced by utilizing vectored lift. Figure 13 summarizes takeoff performance of the X-29 and X-29/ADEN and clearly shows the substantial payoff provided by the vectorable nozzle.

With the added feature of a variable thrust axis, the analysis of X-29/ADEN takeoff characteristics included determination of the VEER setting during the acceleration phase of the ground run. The results show that maximum longitudinal force is obtained with some upward deflection of the VEER, based on the ADEN static test data at sea level. For a maximum power takeoff, the VEER should be set at −5 deg for best acceleration; for an intermediate power takeoff, a −3 deg VEER setting is optimum. These VEER angles correspond to −2.4 and −7 deg of thrust deflection, respectively.

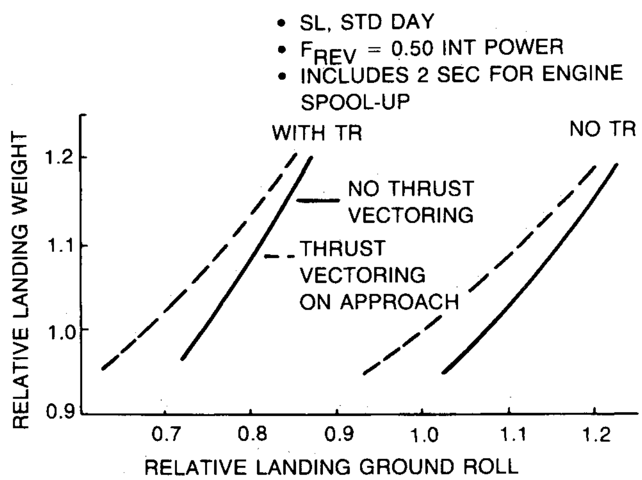

Fig. 15 Effect of thrust reversal on landing distance.

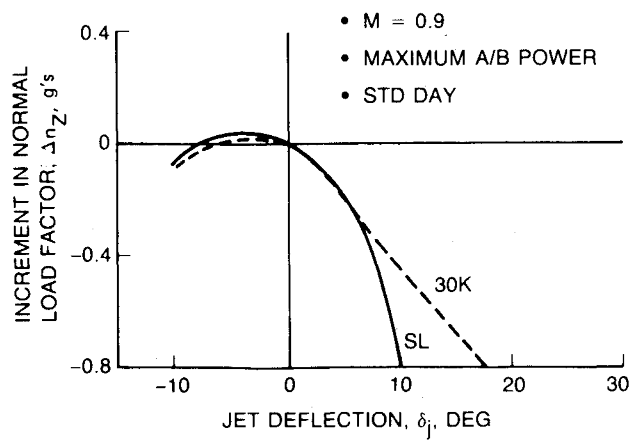

Fig. 16 Effect of thrust vectoring on sustained maneuver *g* capability.

Approach/Landing

Small improvements in approach speed are possible with incorporation of the ADEN. Figure 14 depicts the effect of thrust deflection on X-29/ADEN power approach characteristics on a 3 deg glide slope at an angle of attack of 12 deg. The power setting during approach is approximately one-third intermediate thrust. The existing canard is capable of trimming out up to 13 deg of deflected thrust with the wing flap positioned at the 25 deg position. The added lift from 11 deg of thrust deflection, which provides some margin to canard saturation, results in an approach speed reduction of 4.6% and a landing distance decrease of 6.5%. A flaps 0 deg approach allows for a 30 deg VEER angle to be demonstrated, due to the load relief on the canard.

Installation of a thrust reverser on the X-29/ADEN results in STOL-like landing performance. Figure 15 shows the relative ground roll distance vs relative landing weight for the X-29/ADEN with and without reverse thrust capability. The calculated field lengths are based on 50% reverser effectiveness and assume an interval of 2 s from touchdown to full braking and reversing. During this time, the aircraft is pitched down until the nosewheel contacts the ground and the engine spools up to intermediate power. The reverser is used only until the vehicle decelerates to 40 knots, due to exhaust reingestion considerations. The plot shows that thrust reversal reduces the ground roll by approximately 30%.

Maneuver Turn Capability

Figure 16 shows that thrust vectoring provides no improvement to X-29 sustained maneuvering performance at 0.9 Mach

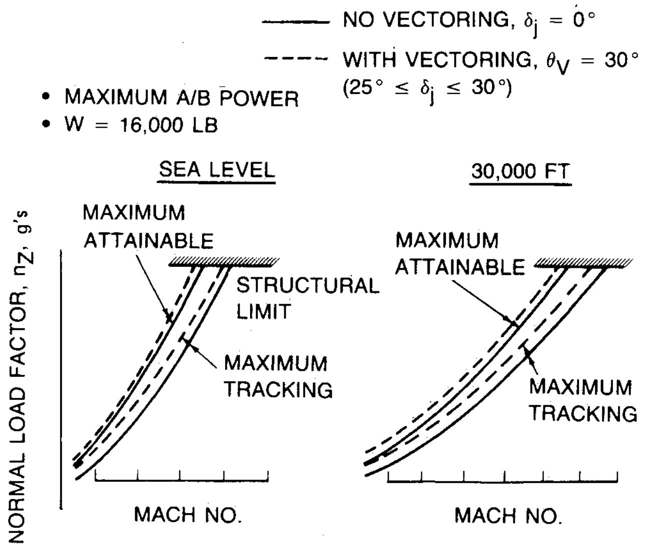

Fig. 17 Effect of thrust vectoring on instantaneous load factor.

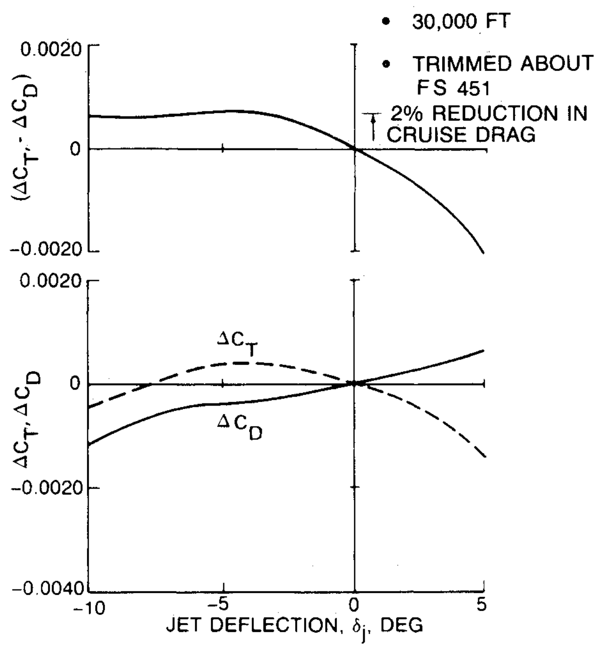

Fig. 18 Effect of thrust vectoring on cruise trim drag, $M = 0.8$.

number. (Similar results were demonstrated for a high-performance aircraft with thrust vectoring in Ref. 11.) Additional analyses conducted at other Mach numbers indicate findings similar to those presented in Fig. 16. Use of thrust vectoring to enhance sustained maneuver capability can be favorable to aircraft, with high wing loadings and/or unsophisticated wing designs, by improving the shape of the drag polar above angles of attack where significant flow deterioration occurs on the wing. Induced effects from supercirculation can add further to high lift efficiency with vectored thrust on appropriately configured aircraft. The X-29 wing with its variable camber, thin supercritical airfoil, and forward sweep was designed for high-g, transonic maneuvering and because of its high efficiency precludes a "crossover" of individual vectored thrust polars.

The increase in maximum attainable lift from vectored thrust translates into improved, instantaneous maneuvering performance. Figure 17 shows an increase in g level at both sea level and 30,000 ft with maximum VEER deflection. The propulsive lift gain at constant angle of attack also improves maximum usable (i.e., moderate wing buffet) performance (see Fig. 17).

Subsonic, Supersonic Cruise

Improvements in cruise trim drag, both subsonic and supersonic, are offered by thrust vectoring. Calculations were made at an altitude of 30,000 ft and Mach numbers of 0.8 and 1.2. The subsonic results are shown in Fig. 18. The graph depicts the effect of thrust deflection on the change in net thrust along the flight path direction (ΔC_T) and on the incremental change in trimmed drag coefficient (ΔC_D). The difference of these two terms represents the net effect of vectored thrust on total aircraft drag. The 2% drag reduction at $M = 0.8$ and a 1% reduction at $M = 1.2$ that occur with 3 deg of upward jet deflection can be interpreted as reductions in thrust required and, therefore, decreases in fuel flow. These reductions are largely a consequence of the present X-29 control surface schedule (i.e., canard, wing flaps, and aft fuselage strake flap), optimized for minimum drag without power effects.

Conclusions

The study, which included a detailed hardware installation assessment together with a performance evaluation, demonstrated the feasibility of incorporating the ADEN nozzle into the X-29 aircraft, and also several performance benefits. These included: 28% decrease in takeoff speed, 48% decrease in takeoff ground roll, 4.5% decrease in approach speed, 7% decrease in landing ground roll, and 4% increase in instantaneous turn rate.

Incorporation of a thrust reverser provides a 30% reduction in landing distance in addition to the tactical advantages that would be provided with in-flight deceleration.

Analysis of the aft-end drag demonstrated lower drag levels for the ADEN than the axisymmetric nozzle for both intermediate and maximum A/B power settings.

Acknowledgments

This study was performed under Contract MDA 903-82-C-0218 from the Defense Advanced Research Projects Agency.

The author wishes to acknowledge the effort of several key personnel in this program: B. Kock of NASA Dryden, the Program Manager; F. Markil, the Grumman Study Manager; J. Landfield, responsible for the study aerodynamics; R. Mercadante, who performed the many computer runs for the aft-end drag determination; and W. Wooten of GE, who provided the ADEN nozzle hardware characteristics and performance.

References

[1]Wooten, W.H., Blozy, J.T., Speir, D.W., and Lottig, R.A., "Altitude Testing of a Flight Weight, Self-Cooled, 2D Thrust Vectoring Exhaust Nozzle," SAE Paper 841557, Oct. 1984.

[2]Markil, F.S., Landfield, J.P., Klafin, J., Miller, E.H., Reichel, H., and Wooten, W., "Non-Axisymmetric Nozzle Flight Demonstrator Feasibility Study on FSW X-29 Aircraft," Defense Advanced Research Projects Agency, Rept. MDA 903-82-C-0218-100, Dec. 1982.

[3]Miller, E.H., "Performance of a Forward Swept Wing Fighter Utilizing Thrust Vectoring," AIAA Paper 83-2482, Oct. 1983.

[4]Spacht, G., "The Forward Swept Wing: A Unique Design Challenge," AIAA Paper 80-1885, Aug. 1980.

[5]Spacht, G., "X-29 Integrated Technology Demonstrator and ATF," AIAA Paper 83-1058, March 1983.

[6]Davis, W.H. Jr., "Analysis of Isolated Subsonic-Transonic Boattails in the Presence of Separation and Exhaust Plume Entrainment," Grumman Aerospace Corp., Bethpage, NY, Propulsion Rept. PXP-001-55, Sept. 1978.

[7]August, R.A., "Analysis of Isolated Supersonic Boattails Including Plume and Viscosity Effects," Grumman Aerospace Corp., Bethpage, NY, Propulsion Rept. PXP-001-56, July 1980.

[8]Mercadante, R., "Supersonic Boattail Analysis, P21," Grumman Aerospace Corp., Bethpage, NY, Rept. EG/RAVES-UM-405-82, Sept. 1982.

[9]Capone, F.J., Hunt, B.L., and Poth, G.E., "Subsonic/Supersonic Nonvectored Aeropropulsive Characteristics of Nonaxisymmetric Nozzles Installed on an F-18 Model," AIAA Paper 81-1445, July 1981.

[10]Capone, F.J., "Aeropropulsive Characteristics at Mach Numbers Up to 2.2 of Axisymmetric and Nonaxisymmetric Nozzles Installed on an F-18 Model," NASA TP 2044, Aug. 1982.

[11]Miller, E. and Protopapas, J., "Nozzle Design and Integration in an Advanced Supersonic Fighter," AIAA Paper 79-1813, Aug. 1979.